

Luminosity limits for liquid argon calorimetry

Rutherford J and Walker RB

Physics Department, University of Arizona, Tucson, Arizona 85721

E-mail: rutherford@physics.arizona.edu

Abstract. We have irradiated liquid argon ionization chambers with betas using high-activity Strontium-90 sources. The radiation environment is comparable to that in the liquid argon calorimeters which are part of the ATLAS detector installed at CERN's Large Hadron Collider. We measure the ionization current over a wide range of applied potential for two different source activities and for three different chamber gaps. These studies provide operating experience at exceptionally high ionization rates. We can operate these chambers either in the normal mode or in the space-charge limited regime and thereby determine the transition point between the two. From the transition point we indirectly extract the positive argon ion mobility.

1. Introduction

The liquid argon sampling calorimeters in the ATLAS detector [1] collect the ionization produced in the argon by penetrating, high energy charged particles. Most of these high energy charged particles within the calorimeter are in electromagnetic or hadronic showers produced by a higher energy particle incident on the face of the calorimeter. These incident particles typically come from one of the copious min-bias proton-proton collisions produced by CERN's Large Hadron Collider (LHC) [2]. At the LHC design energy and luminosity there are of order 100 particles produced in each min-bias proton-proton collision and these collisions come at a rate of almost 1 GHz. The number of charged particles above a kinetic energy of 1 MeV in a typical shower varies with depth in the calorimeter, reaching many tens at shower maximum. At small angles ($\sim 1^\circ$) to the incident proton beams at an instantaneous luminosity of $5 \times 10^{34} \text{ cm}^{-2} \text{ s}^{-1}$ (as proposed for the high luminosity upgrade of the LHC, the HL-LHC) at about 5 m from the interaction point there will be about one gamma of average energy about 15 GeV per square centimeter per 25 ns crossing incident on the face of the calorimeter. The ionization rate in a liquid argon gap located at electromagnetic shower maximum is about $3 \times 10^{11} \text{ /mm}^3/\text{s}$.

The liquid argon ionization chambers, distributed within a metal matrix, are made up of two electrodes separated by a gap of about 2 mm in most of the ATLAS calorimeters. But in the forward direction where the energy and density of particles incident on the face of the calorimeter are highest, the gaps are much smaller, approximately 0.27 mm at depths up to hadronic shower maximum. For either gap the applied electrical potential is adjusted to give an electric field within the gap of approximately 1000 V/mm. At this electric field the ionization electrons drift at a speed of about $4.3 \times 10^6 \text{ mm/s}$ and the positive argon ions drift in the opposite direction at about 100 mm/s. So for the 0.27 mm gap an ionization electron takes about 63 ns to drift from one electrode to the other while the positive argon ion takes about 2.7 ms. On the scale of the gap size this ionization is roughly spatially uniform. And on the scale of ion drift times the

current drawn from the high voltage power supply due to this ionization is roughly constant in time.

2. Phenomenology

High energy charged particles passing through the liquid argon shake loose outer shell electrons from those argon atoms close to the particle track. Without an electric field, the ionization electron would likely recombine with its argon ion. But with an electric field the ionization electrons may escape and drift freely in the liquid argon. Measurements [3] give the average energy loss of the charged particle in liquid argon required to create one electron-ion pair as $W = 23.6^{+0.5}_{-0.3}$ eV at an electric field of 22 kV/cm. This gives about 9000 ionization electrons per mm of track.

Several forms of recombination deplete the ionization electrons. We will divide these forms into two classes. In the first category ionization electrons recombine with their corresponding ion or with other ions produced by the same particle track. This form of recombination is independent of the number of tracks in the chamber and dominates when the tracks are widely separated in space and/or time. In the second category the ionization electrons recombine with ions produced by a different particle track. This “bulk” recombination is proportional to the density of ionization electrons and ions and dominates at high ionization rates.

At such high ionization rates the slowly-drifting positive argon ions build up in the liquid argon gap enough to distort the electric field [4]. At the critical ionization rate D_c the distortion is so large that the electric field is almost completely screened next to the anode. In this case the normally fast-drifting electrons also slow so much that they accumulate in this region next to the anode. As the ionization rate increases above this critical value the screened region near the anode, with its accumulation of electrons, expands toward the cathode. The density of positive argon ions equals the density of ionization electrons in this region and they recombine at the same rate they are produced.

As is usual, we will assume the drift velocity of the positive argon ions is given by

$$v_+ = \mu_+ E \quad (1)$$

where μ_+ , the positive ion mobility, is independent of electric field E . In this case the critical ionization rate is given by

$$D_c = \frac{4V_0^2 \epsilon \mu_+}{ea^4} \quad (2)$$

where V_0 is the electrical potential across the gap, ϵ is the permittivity of liquid argon, e is the magnitude of the electron charge, and a is the gap width, i.e. the distance from anode to cathode. The units of D_c are the number of electron-ion pairs produced in the liquid argon per unit volume per unit time. Note that D_c increases as the gap width decreases, allowing the chamber to operate normally at higher rates. We next define D_i as the actual ionization rate. This is proportional to the flux of high energy particles in the liquid argon gap. And finally we define the *relative* ionization rate

$$r = \frac{D_i}{D_c} \quad (3)$$

The value of the positive ion mobility μ_+ is not well known. As explained in reference [4] there are large inconsistencies in the many measurements of μ_+ reported in the literature.

3. The measurement

In order to determine the threshold ionization rate D_c separating the normal operating regime from the space-charge limited regime, we designed a liquid argon ionization chamber with an argon volume which is approximately uniformly illuminated by betas as shown in Fig. 1. Two

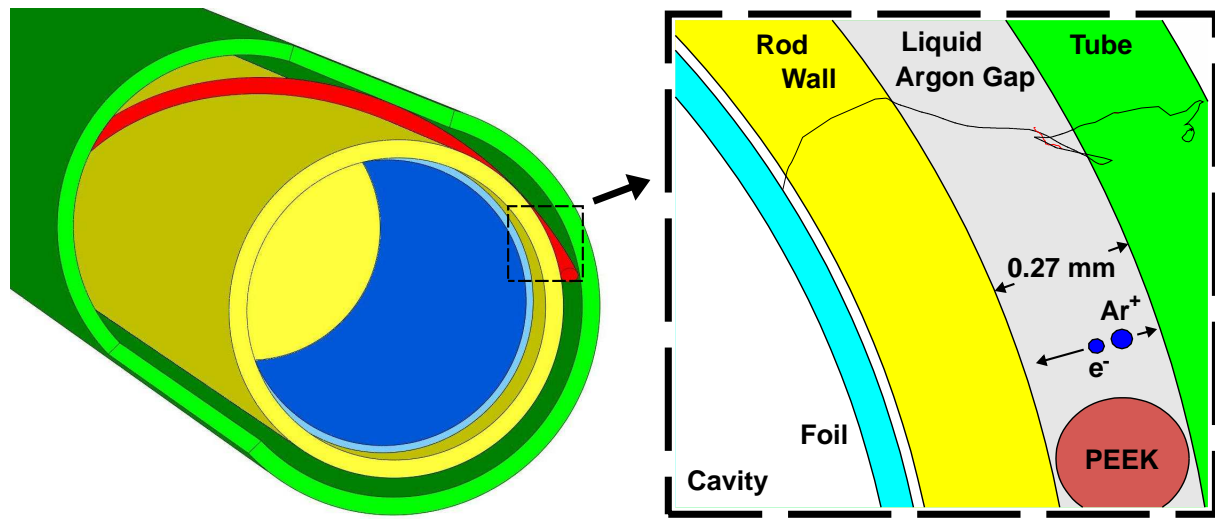


Figure 1. Liquid argon ionization chamber with Strontium-90 beta source. The perspective drawing on the left shows a cut-away of the two electrodes: a copper rod (yellow) within a thin-walled copper tube (green). The rod is held in place within the tube by an insulating PEEK fiber (red) wound helically around the rod. The gap between the rod and tube fills with liquid argon forming the ionization chamber. The solid copper rod of diameter 4.712 mm has a concentric cavity of diameter 4.212 mm machined out to a depth, along the axis of the rod, of 14 mm. Inserted into this cavity is a rolled copper foil (blue) of 10 mm length, coated on the outer surface with the Strontium-90 beta source. The open end of this rod is then welded to another solid copper rod (not shown), making one rod of longer length. The drawing on the right shows a cross-sectional close-up of this structure. Overlaid is the track of one simulated beta, from the Yttrium decay product of a Strontium-90 decay, leaving the source on the surface of the foil with kinetic energy of 1.48 MeV and passing through the liquid argon gap. An energetic delta ray, produced in the liquid argon, is represented by the red track.

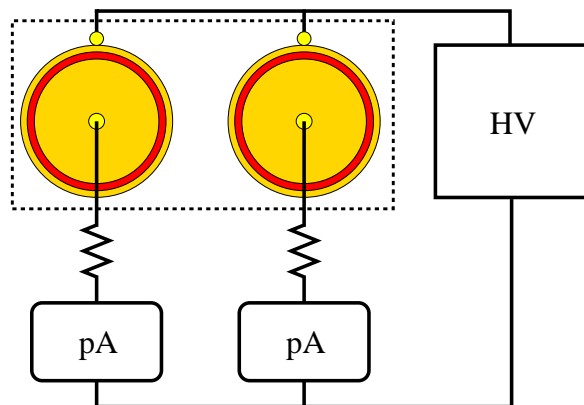


Figure 2. Schematic current readout circuit. Shown at the signal connection end are two ionization chambers with copper parts in yellow and liquid argon in red. HV is the high voltage power supply which places a potential between the rod and tube and each pA is a picoAmmeter. The resistors are $4\text{ M}\Omega$ for the 50 mCi source and $10\text{ M}\Omega$ for the 2 mCi source. The currents we measure are so small that the potential drop across each resistor is almost negligible.

rods containing beta sources were produced, one specified at 50 mCi and the other at 2 mCi. The ratio of activities turned out to be 21.37 rather than the expected value of 25. Tubes of three different inner radii were used at different times during this measurement to give liquid argon gaps of three different widths. An electric potential across the electrodes causes the charges in the intervening liquid argon to drift, inducing a current in an external circuit shown in Fig. 2.

A “data run” consisted of measurements of the currents from the 50 mCi and the 2 mCi

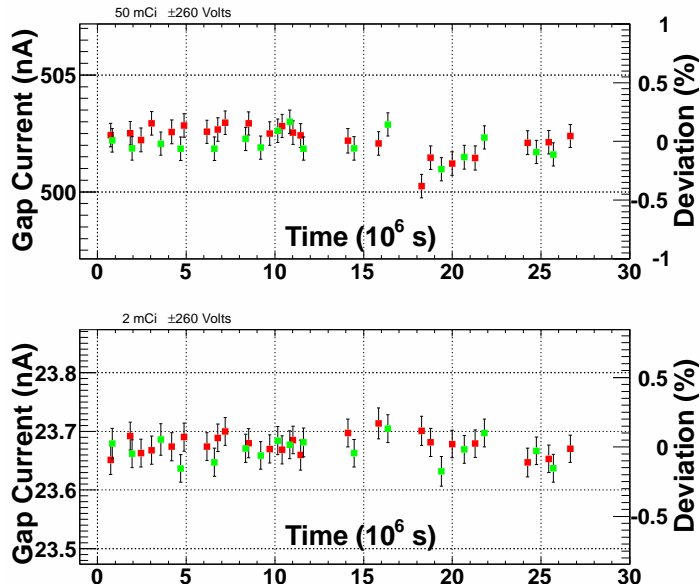


Figure 3. Currents in the $268 \mu\text{m}$ ionization chambers at the operating potential of 260 V as a function of time of the run, after correction for the decay of the beta sources. Red (green) data points are at positive (negative) polarity. This potential corresponds to the standard electric field of approximately 1000 V/mm used in the ATLAS liquid argon calorimeters.

chambers with the same gap width at a series of closely-spaced values of the potential across the electrodes. Each run lasted between 3 and 8 hours. Eight runs, each with a different HV power supply, were required to cover the full range of potentials at both polarities. A “fill” refers to the filling of our cryostat with liquid argon and operating it during a series of runs with the two chambers of a given gap width. Runs were repeated many times during a fill to check for reproducibility. These runs were interspersed with runs to test for various small effects like the very small leakage of radiation from the 50 mCi chamber into the 2 mCi chamber. There were three fills in all and between fills the tubes were changed to give different gap widths. Fills lasted several months, the longest being a little over 10 months.

Fig. 3 shows measurements of the chamber currents at a potential of 260 V when using $268 \mu\text{m}$ gaps during the long 10-month fill (about 2.7×10^7 seconds). For the 50 mCi chamber this is approximately equivalent to the exposure experienced by one of the ATLAS forward calorimeter ionization chambers at a depth in the calorimeter near electromagnetic shower maximum at an angle to the LHC proton beam of 1.04° for an integrated luminosity of about 500 fb^{-1} . Over this 10-month period the activity of the Strontium-90 sources (half life of about 29 years) dropped by about 2%. The currents shown here are corrected for this effect. The corrected currents are stable at a level of approximately 0.1%. This result suggests that the liquid argon technology as the sensitive medium of a sampling calorimeter is a good choice for experiments operating at very high intensities.

To map out the behavior of liquid argon ionization chambers as they are driven into the space-charge limited regime we would ideally vary the ionization rate by varying the activity of the beta sources. But with only two different source activities we were forced to adopt a different strategy. This alternate approach is based on the observation that the critical ionization rate D_c depends on the potential V_0 applied across the two electrodes. Rather than varying D_i (by varying the source activity) we, instead, vary D_c (by varying V_0). But in varying V_0 we not only change D_c we also change D_i , a potential complication.

However, if we divide the currents from the 50 mCi chamber by the currents from the 2 mCi chamber we cancel effects which are not rate-dependent and make manifest those effects which are rate-dependent, at least for potentials above the point where the 2 mCi chamber enters the space-charge limited regime.

4. Interpretation of the data

Fig. 4 shows the currents as a function of the potential applied across the gaps for one of the three gap widths. The currents from the 2 mCi chamber have been multiplied by 21.37 for comparison with the currents from the 50 mCi source. Such data is referred to as a High Voltage Plateau Curve because the current “plateaus” to a relatively constant value at higher values of potential. It is interesting that this data shows a very slow rise with potential over the full high end of the range we were able to cover. That is, there is no evidence that the current actually becomes constant at high potentials.

For potentials above about 100 V the currents from the 2 mCi and 50 mCi chambers have the same shape. This is the range in which both chambers are operating in the normal regime. Below about 100 V the 50 mCi chamber goes into the space-charge limited regime. This can be seen better in Fig. 5 where the ratios of the currents are shown for all three gap widths. At the higher values of potential both chambers, at a given gap width, are operating in the normal regime. Going down in potential, the 50 mCi chamber first enters the space-charge limited regime where the ratio falls off. Eventually the 2 mCi chamber also enters the space-charge limited regime where the ratio approximately levels off again. As predicted by Eq. 2 the potential of the critical ionization rate varies with the gap width. A simplified analytic approximation superimposed on the ratio data shows qualitative agreement. This simplified calculation predicts the ratio at low potentials will be the 3/4ths power of the ratio at the high potentials.

The simple predictions shift left and right depending on the value assumed for the positive

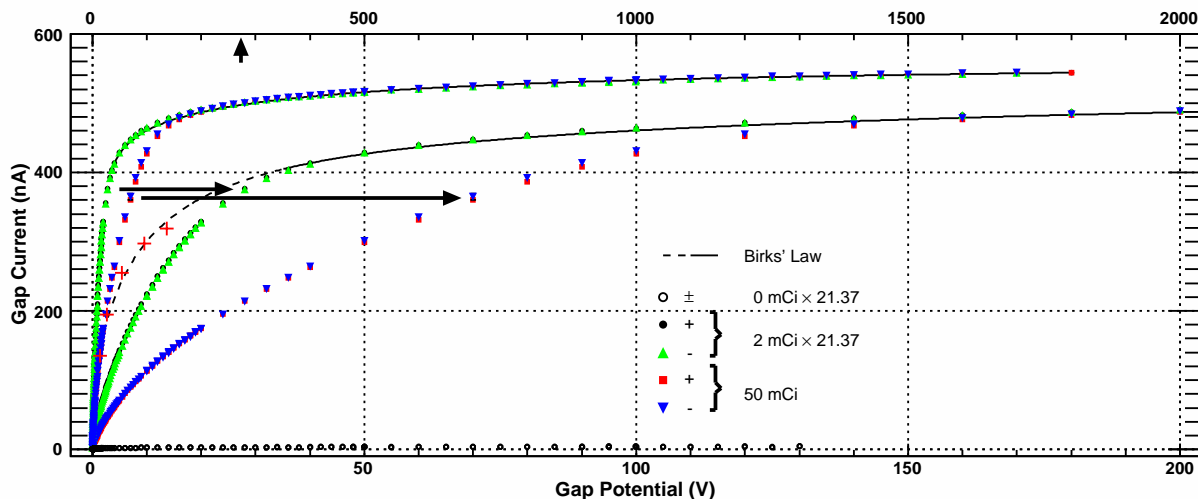


Figure 4. Currents from the ionization chambers with 268 μm gaps versus the applied potential. Both polarities are shown. Absolute values are taken for the negative currents and potentials. For potentials at and below 200 V the data points are plotted twice, once using the potential axis at the bottom of the plot and once using the potential axis at the top of the plot. Horizontal arrows connect two example pairs of identical data points. For potentials above 200 V data points are plotted only once using the axis at the top. The currents from the 2 mCi ionization chamber are multiplied by 21.37 to show how the currents agree in shape at higher potentials. The currents from the 0 mCi ionization chamber, multiplied by 21.37, are also shown. A Birk's Law [5] inspired parameterization is represented by the solid curve in the region of potential where the data was fit. This parameterization, extrapolated to lower potentials, is shown as a dashed line. A vertical arrow on the top axis shows the nominal operating potential in the ATLAS detector.

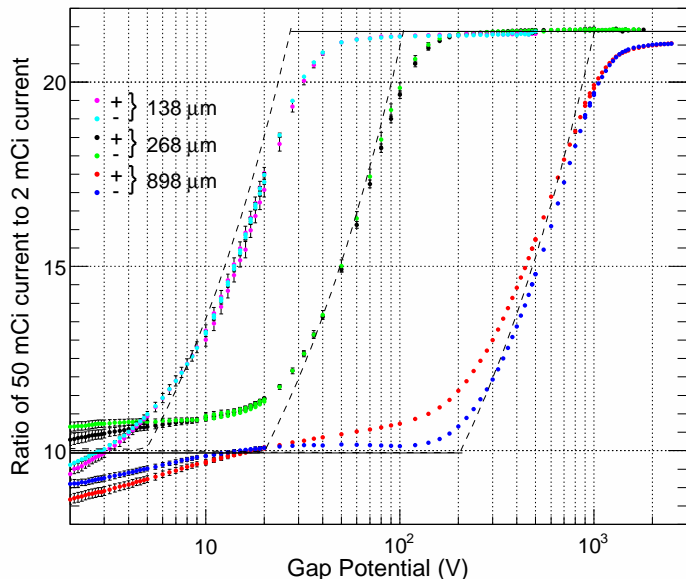


Figure 5. Ratio of the 50 mCi chamber currents to the 2 mCi chamber currents as a function of the potential across the ionization chamber for, from left to right, the 138 μm gap, the 268 μm gap, and the 898 μm gap. Data for the two polarities of potential are shown separately as indicated in the key. A simple analytic approximation is shown by dashed curves.

argon ion mobility μ_+ . The value chosen for the plot in Fig. 5 is $\mu_+ = 0.10 \text{ mm}^2/\text{V}\cdot\text{s}$. At this time we assign an rms error of $\pm 0.02 \text{ mm}^2/\text{V}\cdot\text{s}$ dominated by uncertainties in the simple analytic approximation. We have written a detailed numerical simulation program with all the effects we can imagine might play a role. Many of the parameters governing these effects have not been measured at all or not measured over the range of electric fields covered by our data so we are trying to determine the sensitivity of the data to these unknown parameters and their correlations.

5. Summary

Using a strong-activity beta source distributed uniformly across a large-area foil we have exposed liquid argon chambers to ionization equivalent to the worst location in the ATLAS calorimeter system at luminosities approximately a factor two above the LHC design value. A weaker source acted as a control. We found that the chamber currents were stable at the 0.1% level during very long runs. This bodes well for prolonged running at the LHC design luminosity and a little above.

By varying the electrical potential across the liquid argon ionization chambers we were able to operate these chambers in the normal operating regime or in the space-charge limited regime. The ratio of currents from the 50 mCi chamber to currents from the 2 mCi chamber cancelled out effects which are rate independent leaving a measure of rate dependent effects. Using simple analytic approximations we estimate the potential which separates the normal regime from the space-charge limited regime and extract a value for the positive argon ion mobility of $0.10 \pm 0.02 \text{ mm}^2/\text{V}\cdot\text{s}$. The error includes an estimate of uncertainties introduced by the simple analytic approximation. Full simulations, when completed, should allow smaller uncertainties.

6. References

- [1] ATLAS Collaboration, *The ATLAS Experiment at the CERN Large Hadron Collider*, 2008 JINST 3 S08003.
- [2] Lyndon Evans and Philip Bryant (editors), *LHC Machine*, 2008 JINST 3 S08001.
- [3] Miyajima M, Takahashi T, Konno S, Hamada T, Kubota S, Shibamura H, and Doke T, *Average energy expended per ion pair in liquid argon*, 1974 Phys. Rev. A 9 1438 and Erratum in 1974 Phys. Rev. A 10 1452.
- [4] J.Rutherford, *Signal degradation due to charge buildup in noble liquid ionization calorimeters*, Nucl. Instr. and Meth. A482 (2002) 156 and references therein.
- [5] J.Birks, *Theory and Practice of Scintillation Counting*, Pergamon Press, 1964.